Cooperative Adsorption Behavior of Fatty Acid Methyl Esters from Hexadecane *via* Coefficient of Friction Measurements

Todd L. Kurth[a,*], Girma Biresaw[a], and Atanu Adhvaryu[b]

[a]Cereal Products and Food Science Research Unit, NCAUR, ARS, USDA, Peoria, Illinois 61604, and [b]Department of Chemical Engineering, Pennsylvania State University, University Park, Pennsylvania 16802

ABSTRACT: The frictional behaviors of methyl oleate (MO), methyl palmitate (MP), methyl laurate (ML), and methyl stearate (MSt) as additives in hexadecane have been examined in a boundary lubrication test regime using steel contacts. It was found that the transient attributes of coefficient of friction (COF)–time spectra are a sensitive measure of adsorption equilibria. Critical additive concentrations were defined and used to perform novel and simple Langmuir analyses that provide an order of adsorption energies: MSt > MP > MO ≥ ML. Application of Langmuir, Temkin, and Frumkin–Fowler–Guggenheim adsorption models *via* nonlinear fitting of a general cooperative model demonstrates the necessary inclusion of cooperative effects in the applied model. In agreement with the qualitative features of steady-state COF–concentration plots, MSt modeling requires minimal cooperative interaction terms. However, MO, MP, and ML data require large attractive interaction terms to be adequately fitted. Primary adsorption energies calculated *via* the cooperative model are necessarily decreased, whereas total adsorption energies correlate well with values obtained *via* critical concentration analyses. These results and comparisons with previous adsorption studies of MO and MSt suggest that primary (ester-surface) and secondary (alkyl-surface) adsorbate–adsorbent, adsorbate–adsorbate, and (free-additive) adsorpt–adsorpt interactions collectively determine both the calculated primary and the cooperative interaction energies.

Paper no. J11008 in *JAOCS 82*, 293–299 (April 2005).

KEY WORDS: Adsorption, ball-on-disk, boundary lubrication, FFG, friction, isotherm, Langmuir, Temkin.

Biobased replacements for petroleum-based materials are currently being sought for a variety of industrial uses (1). Owing to their amphiphilic character, naturally occurring TG and their derivatives are ideally suited for boundary lubrication applications (2). Critical to their performance is the ability to adsorb to a metal surface. Members of our laboratory previously worked to quantify and contrast the adsorption properties of a series of plant oils as additives in a ball-on-disk boundary lubrication test geometry (3,4). Langmuir and linearized Temkin analyses were applied to isothermal coefficient of friction (COF)-derived adsorption data for additive/hexadecane solutions. As we continue to develop and apply this methodology to a wide range of biobased lubricant systems, we seek to increase our understanding of the fundamental structure–property relationships of simpler model systems. Because FAME present the simplest analogs of the complex TG mixtures found in plant oils, we have chosen to examine their frictional behavior as additives in the boundary lubrication regime. These more easily described systems yield insight into specific intermolecular interactions relevant to tribophysical and tribochemical processes.

Rowe (5) defined the complex relationship between frictional wear rate in a boundary lubrication regime and additive concentration (for a two-component lubricant). Inherent in his model is the relationship of additive surface coverage (θ) to additive concentration (C). For this, he relied on the Langmuir adsorption isotherm (6,7):

$$\theta = \frac{KC}{1+KC} \quad [1]$$

This equation is defined by the equilibrium conditions of a two-state reaction. K is the association equilibrium constant:

$$K = e^{-E_{ads}/RT} \quad [2]$$

Thus, more strongly adsorbing additives lead to more negative adsorption energies, E_{ads}.

Jahanmir and Beltzer (8) used similar methodology to relate COF in the boundary lubrication regime to additive concentration. They also used the Langmuir model, and the relationship between COF and surface coverage for one-additive systems was defined (8,9):

$$f = f_b(1-\theta) + f_a\theta \quad [3]$$

where f is the measured COF, f_a is the measured COF at high additive concentration, and f_b is the measured COF in pure base lubricant. The coefficients of the linear combination are the fractional surface coverages of the respective lubricant component. Rearrangement of this equation allows the determination of θ directly from friction measurements:

$$\theta = \frac{f-f_b}{f_a-f_b} \quad [4]$$

*To whom correspondence should be addressed at USDA, NCAUR, CPF, 1815 N. University St., Peoria, IL 61604. E-mail: kurtht@ncaur.usda.gov

Current address of third author: Technology and Solutions Division, Caterpillar Inc., Peoria, IL 61656.

These θ and the Langmuir model permit the determination of K and thus E_{ads} *via* linear plots:

$$\frac{1}{\theta} = \frac{1}{K}\frac{1}{C} + 1 \quad [5]$$

Jahanmir and Beltzer (8) noted the importance of cooperative (lateral interaction) effects on adsorption, which is unaccounted for in the Langmuir model. To incorporate such effects, those authors utilized a linearized Temkin model, which assumes by its application only repulsive cooperative interactions, $\alpha > 0$, and a primary adsorption energy, E (8,10):

$$E_{ads} = E + \alpha\theta \quad [6]$$

A model treating attractive cooperative interactions, termed Frumkin–Fowler–Guggenheim (FFG), also has been defined and applied to adsorption data (11). It has the same form as the Temkin equation, where n is the number of interacting molecules and Q is the attractive lateral (cooperative) interaction energy ($Q < 0$):

$$E_{ads} = E + nQ\theta = E + RT\beta\theta \quad [7]$$

For simplicity of application nQ/RT is traditionally defined as β. One may observe that the Langmuir, Temkin, and FFG models are essentially identical if the cooperative interaction terms are allowed to be zero, positive, or negative ($\alpha/RT = nQ/RT = \beta$; see Fig. 1):

$$K = e^{-(E+\alpha\theta)/RT} = e^{-(E+nQ\theta)/RT} = e^{-E/RT}e^{-\beta\theta} \quad [8]$$

Unfortunately, fitting experimental data with a cooperative effect model (FFG or Temkin) is not straightforward. Unlike the simpler Langmuir model, Equation 8 may not be linearized without simplifying assumptions (10). The necessary assumptions constrain the fitting procedure to independent regions of surface coverage. The values $\theta \le 0.2$, $0.2 \le \theta \le 0.8$, and $1 \ge \theta \ge 0.8$ are fitted by different equations. A "mid-coverage" equation is used almost exclusively for the linearized Temkin analyses (10):

$$\theta = \frac{RT}{\alpha}\ln C - \frac{E}{\alpha} \quad [9]$$

The slopes and y-intercepts of θ vs. ln$C$ plots have been used to determine values of α and E and thus the total adsorption energies *via* Equation 6 (3,4,8). Unfortunately, the primary focus in previous studies was the attainment of E_{ads}, and the cooperative interaction terms were not discussed (3,4,8). Further, reliance on simplified (linearized) models and linear analyses of adsorption isotherms that apply over many orders of magnitude of additive concentration results in a diminished ability to observe and consider subtle but definite nonlinear trends. The limitations of the previous frictional adsorption analyses were an impetus for our application of cooperative adsorption models *via* iterative fitting to a series of FAME COF-derived adsorption isotherms.

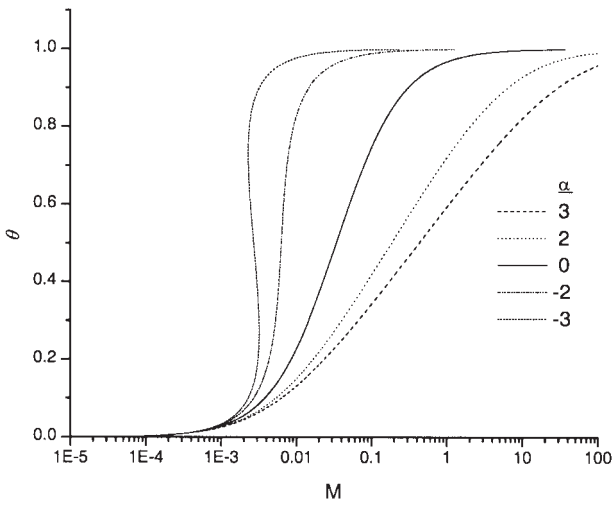

FIG. 1. Cooperative adsorption model (Langmuir α = 0, Temkin α = +, or Frumkin–Fowler–Guggenheim (FFG) α = −): arbitrarily, E = −2 kcal/mol. α is varied from −3 to 3 to simulate the dependence of the model on the cooperative interaction parameter. x-axis, molar concentration; y-axis, θ = additive surface coverage.

EXPERIMENTAL PROCEDURES

Materials. All chemicals were obtained commercially at greater than 99% purity and used as supplied. The lubricant additives were methyl laurate, ML (Sigma, St. Louis, MO), and methyl palmitate, MP, methyl oleate, MO; and methyl stearate, MSt (Aldrich Chemical Company, Milwaukee, WI). The base lubricant was HPLC-grade hexadecane (anhydrous), also from Aldrich. The lubricant formulations constituted 0.0007 to 0.6 M of each additive in hexadecane.

Test specimen. Balls and disks used were obtained commercially (Falex Corporation, Sugar Grove, IL). The specifications of the balls were: 52100 steel; 12.7 mm (0.5 in.) diameter; 64–66 Rc hardness; extreme polish. The specifications of the disks were: 1018 steel; 25.4 mm (1 in.) o.d.; 15–25 Rc hardness; 0.36–0.46 μm (14–18 μin.) roughness. Prior to use, the balls and disks were thoroughly decontaminated by consecutive sonications in fresh HPLC-grade methylene chloride (Aldrich) and HPLC-grade hexanes (Aldrich). It would have been preferable not to use methylene chloride as a solvent due to the potential interactions with the metal surface (12). However, attempts to use isopropyl alcohol led to lower measured COF values for hexadecane (0.38), indicating the presence of impurities from the machining and/or packing process.

Friction test method. Friction was measured under point contact conditions using a ball-on-disk configuration *via* a Falex Friction & Wear Test Machine (Model Multi-Specimen; Falex Corporation). In the ball-on-disk configuration, a ball, in contact with a stationary cylindrical disk, moves in contact around the disk at a specified speed. The resistance to the motion of the ball, i.e., the frictional force (torque), is measured by a load cell connected to the disk. The COF is obtained by dividing the friction force by the normal force pressing the ball

against the disk. The ball was fixed on the upper specimen holder with a point contact radius of 11.9 mm (0.468 in.). The disk was fixed on the lower specimen holder, which is enclosed in a lubricant reservoir. The reservoir was filled with 50 mL of lubricant solution to submerge the ball and disk assembly completely. The disk assembly was then raised and made to contact the ball. The upper specimen was allowed to rotate at 5 rpm (6.22 mm/s). As 5 rpm was reached, load was applied at 50 lb/s to reach 400 lb (181.44 kg). The temperature of the specimen and lubricant throughout each test was 25 ± 2°C. The friction measurements were carried out for 30 min. Repeat trials of additive samples deviated less than 5% from the initial measurement. The COF of pure hexadecane was measured for each additive preparation studied. The average value obtained over 15 tests was 0.44 ± 0.01. Repeat runs of previously used additive samples produced data identical to fresh samples, indicating a lack of chemical reaction.

Scar width measurements. The rotation of the upper specimen (ball) under load and in contact with the lower specimen (disk) ultimately results in a circular wear scar. After each test, scar widths were measured using a Leica StereoZoom 6 (Leica Microsystems, Bannockburn, IL) with digital micrometer attached to the specimen holder (Model 164-162; Mitutoyo, Japan). Four points along the circular track were measured to obtain an average value.

Model fitting procedure. Equations 1 and 8 may be combined and solved for concentration in terms of θ, *E*, and β (10):

$$C = \frac{\theta}{(1-\theta)e^{-E/RT_e - \beta\theta}} \quad [10]$$

This equation is equivalent to the Langmuir, Temkin, and FFG models simultaneously. Application of this general model without constraining β allows the data to determine the necessary sign and magnitude of the cooperative interaction terms without *a priori* assumptions. θ vs. *C* data were fit *via* the optimization of *E* and β using an iterative BFGS (Broyden–Fletcher–Goldfarb–Shanno) quasi-Newton or Nedler–Mead simplex optimization procedure and represent best fits using Matlab (v. 7; Mathworks, Natick, MA). Linear fits (Eqs. 5 and 9) and repeat nonlinear fits of Equation 10 (constrained and unconstrained β) were carried out using the iterative least squares fitting as implemented in Origin (v. 7.5; OriginLab, Northampton, MA). To account for large differences in error magnitude, inverse concentrations were used to provide similar weighting of each data point.

RESULTS AND DISCUSSION

Effect of additive concentration on wear scar. The scars on the ball and disk specimen were examined after each 30-min test. The harder ball specimens showed minimal wear and were not examined extensively. The disks showed a scar width of 3.05 ± 0.03 mm, for all disks, independent of the additive chemistry or concentration in hexadecane. It appears that the disk scar widths are a function of the metallurgy of the specimen and test conditions. The consistency of the disk wear scar indicates equivalent test parameters (e.g., pressure, contact surface area)

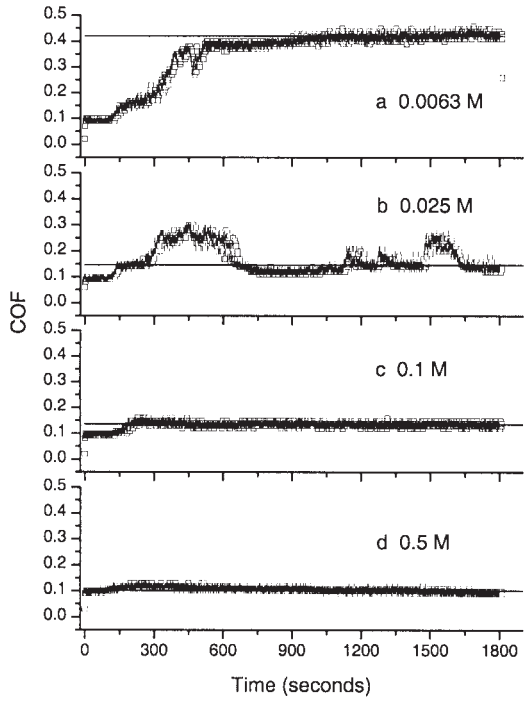

FIG. 2. The methyl oleate (MO) coefficient of friction (COF)–time spectra, shown here, are also representative of methyl palmitate (MP) and methyl laurate (ML): (a) 0.0063 M, (b) 0.025 M, (c) 0.1 M, and (d) 0.5 M in hexadecane. These data were collected *via* a ball-on-disk method.

in the steady-state region. Analogous to ASTM method 5183 for a four-ball COF test (13), these similar contact areas for each COF test are required for quantitative COF comparisons.

COF–time spectra. COF vs. time spectra were generated for each of the methyl esters studied *via* ball-on-disk (e.g., Figs. 2, 3). The MO data are representative of those for MP and ML (analogous MP and ML data were obtained and are not presented here). Shown in Figure 2 are spectra for MO solutions of varying concentration in hexadecane. It is clear that within each spectrum, two regions may be defined: a transient dynamic region and a steady-state region. The dynamic region is characterized by systematic and random variation in COF (wearing-in). The COF variability is attributed to the high initial contact pressure (static load, small variable contact area) and influence of debris formation. As the test progresses, the contact surface area of the ball and softer 1018 steel disk increases to a point at which the pressure is no longer sufficient to cause macroscopic wear and deformation of the softer test specimen. In the steady-state region, nascent surface is maintained with each cycle. Given adequate time (15 min), debris is removed from the circular wear track and the steady-state condition is obtained.

COF–concentration dependence. The COF–time spectrum for 0.00625 M MO in hexadecane, Figure 2a, is characteristic of the lower concentrations and pure hexadecane measured. Figures 2c and 2d (0.1 and 0.5 M, respectively) are characteristic of high concentration data. The spectral responses (time-dependent variations of the data) at low and high concentrations

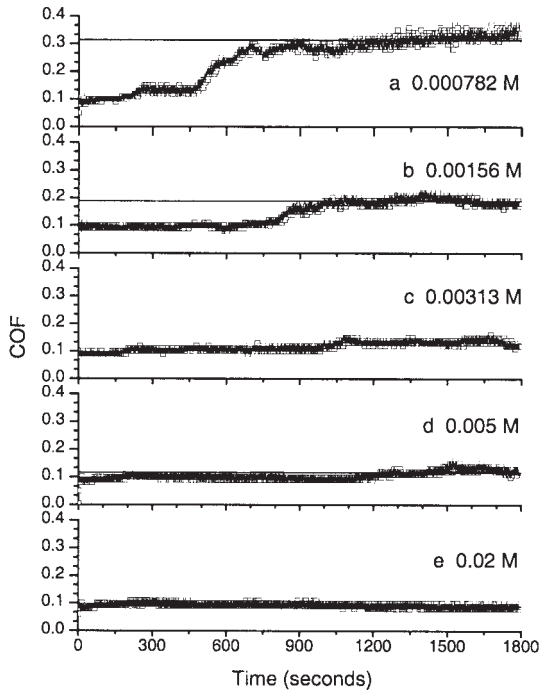

FIG. 3. Methyl stearate (MSt) COF–time spectra: (a) 0.0008 M, (b) 0.0016 M, (c) 0.0031 M, (d) 0.005 M, and (e) 0.02 M in hexadecane. For other abbreviation see Figure 2.

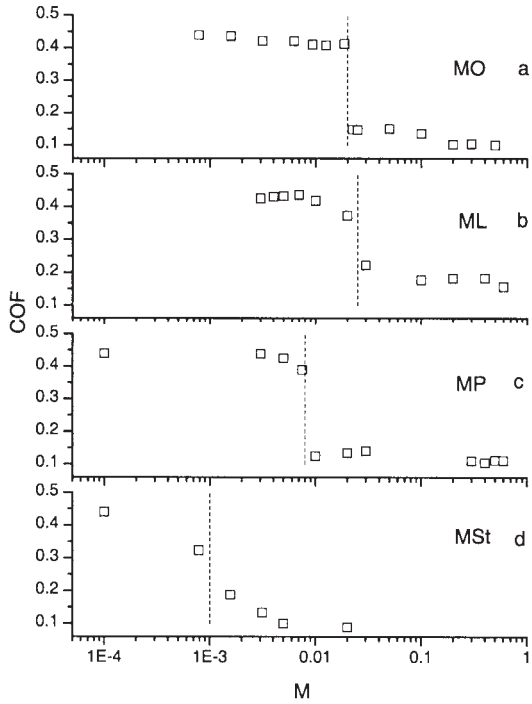

FIG. 4. COF–concentration profiles MO, MP, MSt, and ML. Dashed lines indicate critical concentrations, C_c. For abbreviations see Figures 1–3.

are subtle and continuous (3,4). In each, the wearing-in process occurs, leading to steady-state COF that diminishes with increasing additive concentration. Figure 2b (0.025 M) is a COF–time spectrum characteristic of a "critical" concentration in which the transient wearing-in process is clearly observed with the return to low steady-state COF values. Stick-slip behavior in the steady state is also observed for critical concentrations. Similar behavior and the presence of such critical points of lubricant failure, at low surface coverages, have been noted previously (5,14–17).

In each of the COF–time spectra shown in Figures 2 and 3, the average COF values of the steady-state region data (15–30 min) are indicated by horizontal solid black lines. The concentration-dependent COF behaviors are observable *via* plots of these average steady-state COF values vs. additive concentration (Fig. 4). One may observe the correlation of the critical concentration COF–time spectra (e.g., Fig. 2b) with sharp transitions in the COF-concentration plots for MO, MP, and to a lesser extent, ML (Figs. 4a, 4b, and 4c, respectively).

Figure 4d shows the average steady-state COF vs. concentration data for MSt. These data show that the transition from high to low COF values is not relatively sharp. The presence of a gradual transition (typical of Langmuir behavior) clearly correlates with the COF–time spectral characteristics. The transition (critical) concentrations exhibit wear-in with no return to low COF values and no stick-slip behavior. This allows the prediction of concentration-dependent behavior on observation of the time-dependent COF data, i.e., critical concentration COF–time spectral features are not observed for lubricants that display Langmuir behavior.

Langmuir critical concentration analyses. Critical concentrations, C_c, may be defined as concentrations of additive sufficient to obtain $\theta = 0.5$. These correspond to the inflection points of sigmoidal fits to either COF- or θ-concentration plots. These are depicted in Figure 4 by vertical dashed lines, from which one may quantify the trend in critical concentration: MSt < MP < MO ≤ ML (Table 1). Several researchers (5,14–17) reported that such critical regions are defined by the surface coverage (adsorbate concentration) at which sufficient asperity separation occurs. In the previous work, the Langmuir model was used to define critical temperatures (at high concentration) for additive lubricant failure in the boundary lubrication regime (5,14–17). This is directly analogous to our work in that temperature and/or concentration may be varied to affect the steady-state adsorption equilibrium that determines surface coverage. We define an equation relating a critical concentration (at room temperature) to adsorption energy E_c ($\theta_c = 0.5$):

$$-E_c = RT \ln \frac{\theta_c}{(1-\theta_c)C_c} = RT \ln \frac{1}{C_c} \qquad [11]$$

By using $T = 298$ K and $R = 1.987 \times 10^{-3}$ kcal/mol, E_c is obtained from our COF isotherms: MSt, −4.1; MP, −2.8; MO, −2.3; and ML, −2.2 kcal/mol (Table 1). Necessarily, these results correlate with the E_{ads} obtained *via* iterative linear and nonlinear fits of the COF-derived surface coverage data. Thus, the simplicity of calculating E_c directly from the COF-concentration data is preferable.

Nonlinear fitting of adsorption isotherms. The steady-state COF–concentration plots in Figure 4 display clear differences in transition verticality (magnitude of transition slope).

TABLE 1
Friction-Derived Adsorption Data[a]

			Linear Langmuir fits[a]	Nonlinear fits[b]		
Additive	C_c [M]	E_c [c,d]	E_{ads}	β	E	E_{ads} [c]
MSt	0.001	−4.1	−3.8	0	−4.1	−4.1
				−1.3	−3.4	−3.8
MSt (Cu)	0.09	−1.4	−1.3[e]			
			−1.3		—	—
MP	0.009	−2.8	−2.7[g]	−5	−1.3[f]	−2.8
				−6	−1.2	−3.0
MO	0.02	−2.3	−2.9[g]	−5	−1.1[f]	−2.6
				−6	−1.0	−2.8
MO (Cu)	0.03	−2.1	−1.3[e]		—	—
ML	0.023	−2.2	−1.9[g]	−4.0	−1.1[f]	−2.2
				−5	−1.0	−2.5

[a]Adsorption energies are in kcal/mol at 298 K. Data determined by this work unless otherwise noted. [a]Equation 5, [b]Equation 10, [c]θ = 0.5, [d]Equation 11, [e]Jahanmir and (8) Beltzer linear fits, [f]maximal values, [g]Biresaw *et al.* (3,4) linear fits .

Whereas MSt qualitatively appears to exhibit typical Langmuir behavior, MP, ML, and MO indicate varying degrees of transition verticality that are typical of cooperative isotherms (11). A linear Langmuir fit of the MSt surface coverage data was performed (Eq. 5, Fig. 5a). A good correlation was obtained, R^2 = 0.96, resulting in E_{ads} = −3.8 kcal/mol. However, a subtle but clear deviation from linearity is observable. A nonlinear Langmuir fit was also carried out by constraining β = 0 (Eq. 10). The resulting E_{ads} is similar, −4.1 kcal/mol, but the transition verticality of the fit is clearly not sufficient; see β = 0 in Figure 5b. An unconstrained fit of the data provided β = −1.6, E = −3.6 kcal/mol, and thus E_{ads} = −4.0 kcal/mol (Table 1). The small magnitude of β and the similarity of the primary and total adsorption energies are expected from the qualitatively Langmuir appearance of the MSt raw data. Data such as these, which exhibit minimal attractive interaction, no cooperative interaction, or any magnitude of repulsive interaction, are ideally suited to unconstrained iterative fitting with the general model (Eq. 10).

Iterative fitting of the essentially vertical transitions found for MP, MO, and ML is more difficult. Once β is determined to be ≤ −4, larger cooperative interaction terms do not necessarily lead to better fits and thus cannot be quantitatively determined. ML allows the simplest analysis in that an unconstrained fit of Equation 10 yields β = −4.0, E = −1.1 kcal/mol, and thus E_{ads} = −2.2 kcal/mol (Fig. 6a, Table 1). MO and MP have such vertical transitions that only when β ≤ −5 can the data be accounted for (Figs. 6b, 6c). Assuming β = −5 provides maximal E values of −1.1 and −1.3 kcal/mol for MO and MP, respectively. The total adsorption energies (E_{ads}) for ML, MP, and MO agree well with the critical concentration adsorption energies (Table 1). Assuming more negative cooperative interaction terms (β = −6 and −5 for MO and MP, and ML, respectively) does not yield significantly different adsorption energies (Fig. 6, Table 1).

Effect of metal chemistry on adsorption. Adsorption studies using MSt and MO were previously carried out by Jahanmir and Beltzer (8) with copper–copper (Cu–Cu) contacts in a boundary lubrication geometry (ball-on-cylinder). We digitized their published data for purposes of comparison (Fig. 7). The transition verticalities of our steel–steel and their Cu–Cu MSt COF–concentration data are similar, but the critical concentration for Cu–Cu is two orders of magnitude greater. This indicates a dramatically stronger interaction of MSt with the steel surface. By a linear Langmuir analysis, Jahanmir and Beltzer calculated an E_{ads} = −1.3 kcal/mol for MSt adsorption on copper (8). Using

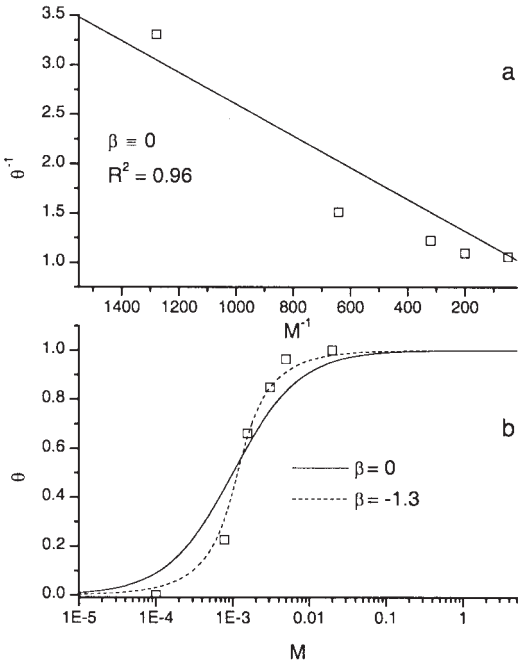

FIG. 5. (a) Linear Langmuir fit of MSt steady-state COF data (Eq. 5), E = −3.8 kcal/mol. (b) Unconstrained nonlinear cooperative model fit, E = −3.4 kcal/mol, β = −1.6 (Eq. 10); and nonlinear representation of linear Langmuir-obtained fit (a).

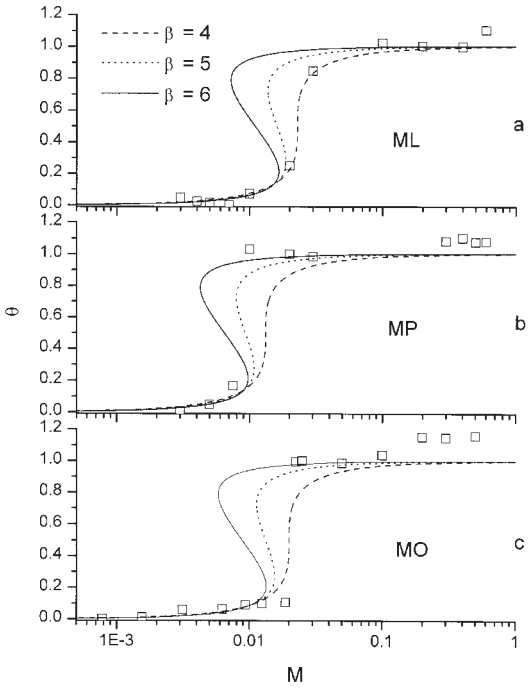

FIG. 6. Cooperative model fits for (a) ML, (b) MP, and (c) MO using β = –4, –5, and –6. For abbreviations see Figure 4.

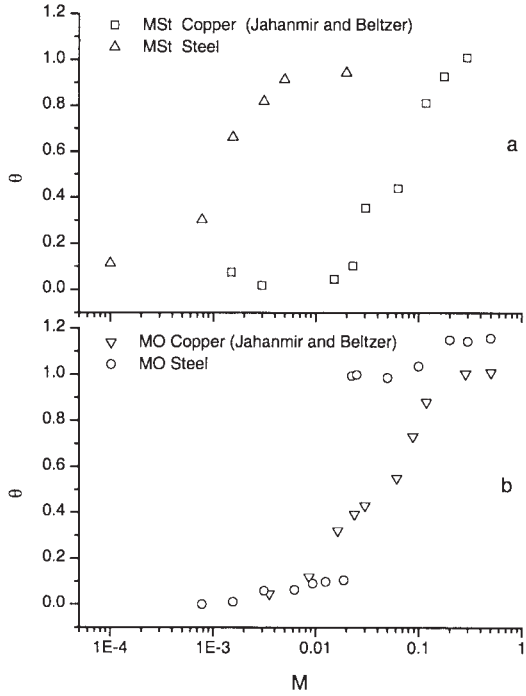

FIG. 7. Comparison of (a) MSt and (b) MO COF–concentration data for steel (this study) and copper (8). For abbreviations see Figures 2 and 4.

their redigitized data and a linear Langmuir analysis, we also calculated $E_{ads} = -1.3$ kcal/mol. However, calculation of an E_c from their data yields a slightly larger value, $E_c = -1.4$ kcal/mol. These are compared with $E_c = -4.1$ kcal/mol for MSt adsorption onto steel. The disparity between the copper and steel data may be explained by the relatively greater activity of the nascent steel surface (18,19) and/or additional test geometry parameters. Factors such as temperature, load, metal hardness, and speed will determine the relative amount of nascent surface and influence the response of the lubricant on the surface. Since both test geometries model boundary lubrication, it is likely that the observed disparities result from the greater activity of the steel surface.

We also compared Jahanmir and Beltzer's MO data for Cu–Cu contacts with our steel–steel data. The MO data indicate similar critical concentrations but not transition verticalities (Fig. 7, Table 1)**.** Contrary to the MSt data, this requires that the primary adsorption energies be similar for MO–steel and MO–copper. A secondary adsorbate–adsorbent (bound additive–surface) interaction of the alkyl chain with the steel surface may explain the more dramatic transition in the MO–steel COF–concentration plot. It is also possible that adsorbate–adsorbate interactions vary with the surface composition, i.e., the primary adsorption (presumably ester–steel interaction) may determine the nature of the cooperative interactions. Conversely, the apparent similarity of the MO–steel and MO–copper interactions may be indicative of the effect of secondary adsorbate–adsorbent interactions on the calculated primary adsorption energy. Further indications of the complex nature of the FAME–steel interaction are observable as subtle transitions at high concentration (Figs. 4, 6). These may be attributable to further cooperative effects at the surface, perhaps between multiple layers.

Cooperative effects. Several authors have proposed that cooperative adsorption isotherms are indicative of the reorganization of previously adsorbed molecules/layers (20,21). With the more active steel surface, it is likely that isolated adsorbates (MO, MP, and ML) have low energy conformations parallel to the metal surface. As subsequent molecules adsorb to the surface, the less energetically favorable parallel interactions are displaced. Although the low concentration equilibrium is determined by solvated additive (adsorpts) and adsorbed parallel additive (adsorbates), the higher-concentration equilibrium conditions are determined by adsorpts and perpendicularly aligned adsorbates. For this reason, a backward-bending function, as in the cooperative model (FFG, Fig. 1, $\alpha = -3$), is expected. In essence, if it were possible to constrain adsorbates to strictly perpendicular or parallel orientations, there would be two different functions, each being similar to the FFG model at low and high concentrations, respectively. An alternative description of the nonphysical region of the FFG model is of a two-phase equilibrium, i.e., "clusters of adsorbed molecules coexist on the surface with single adsorbed molecules, similar to a van der Waals equation of state" (11). In Table 1, the large negative β terms used for fitting the MP, ML, and MO data indicate that cooperative interaction energies dominate the calculated total adsorption energies. Despite this, for clusters of interacting adsorpts (interacting free additives, $n > 2$ in Eq. 7) the lateral interaction energies, Q, may be relatively small in magnitude compared with the adsorption energies, E or E_{ads}.

It has been suggested that MSt is likely to exist as dimers in

solution (15). One may therefore expect MSt to display relatively dramatic lateral/cooperative interaction behavior. Frewing (15) estimated that the dimerization energy for MSt could be about −13 kcal/mol, which would correspond to $\beta \approx -46$ (for $n = 2$). A much smaller value of −1 kcal/mol would still lead to $\beta \approx -4$. Thus, it is not likely that the observed β (−1.3) value corresponds to surface dimerization but rather to relatively minimal interaction of dimers on the steel surface. Adsorption of perpendicularly oriented dimers onto the steel surface would explain the greater adsorption parameter of MSt relative to MP, ML, and MO (15). Such low-energy dimer conformations would also account for the decreased propensity for adsorbate reorganization and the relatively diminished COF–concentration transition verticality on copper or steel (Fig. 4d).

The discrepancy between the copper–MO and steel–MO data requires alkyl–steel interactions (secondary adsorbate–adsorbent interactions) and a relatively large negative cooperative interaction parameter ($\beta < -5$) for MO–steel adsorption. Although the MO data suggest similar primary adsorption mechanisms on copper and steel, the MSt data do not. Thus, equivalent ester moieties of the additives studied require that the fatty alkyl chain interactions vary with the surface composition and contribute not only to the cooperative interaction terms but also to the primary adsorption terms. It is readily observable from the comparisons of the COF-derived methyl ester adsorption parameters (copper and steel) that the calculated primary adsorption and cooperative interaction energies are collective properties of primary and secondary adsorbate–adsorbent (ester–surface, and alkyl–surface, respectively), adsorbate–adsorbate, and adsorpt–adsorpt interactions.

ACKNOWLEDGMENTS

The authors gratefully acknowledge the invaluable contributions of Megan Goers and Armand Loffredo and thank Brajendra K. Sharma for his extensive discussion and assistance. We also thank Sevim Z. Erhan and the Food and Industrial Oil Research Unit (NCAUR) for use of their laboratory and equipment.

REFERENCES

1. Erhan, S.Z., and J.M. Perez, *Biobased Industrial Fluids and Lubricants*, AOCS Press, Champaign, 2002, 135 pp.
2. Bhushan, B., *Introduction to Tribology*, John Wiley & Sons, New York, 2002, 752 pp.
3. Biresaw, G., A. Adhvaryu, and S.Z. Erhan, Friction Properties of Vegetable Oils, *J. Am. Oil Chem. Soc 80*:697–704 (2003).
4. Biresaw, G., A. Adhvaryu, S.Z. Erhan, and C.J. Carriere, Friction and Adsorption Properties of Normal and High-Oleic Soybean Oils, *Ibid. 79*:53–58 (2002).
5. Rowe, C.N., Role of Additive Adsorption in the Mitigation of Wear, *ASLE Trans. 13*:179–188 (1970).
6. Langmuir, I., The Adsorption of Gases on Plane Surfaces of Glass, Mica, and Platinum, *J. Am. Chem. Soc. 40*:1361–1403 (1918).
7. Steinfeld, J.I., J.S. Francisco, and W.L. Hase, *Chemical Kinetics and Dynamics,* Prentice Hall, Upper Saddle River, NJ, 1999, 560 pp.
8. Jahanmir, S., and M. Beltzer, An Adsorption Model for Friction in Boundary Lubrication, *ASLE Trans. 29*:423–430 (1986).
9. Bowden, F.P., J.N. Gregory, and D. Tabor, Lubrication of Metal Surfaces by Fatty Acids, *Nature 156*:97–101 (1945).
10. Brunauer, S., K.S. Love, and R.G. Keenan, Adsorption of Nitrogen and the Mechanism of Ammonia Decomposition Catalysts, *J. Am. Chem. Soc. 64*:751–758 (1942).
11. Butt, H.-J., K. Graf, and M. Kappl, *Physics and Chemistry of Interfaces*, John Wiley & Sons, New York, 2003, 373 pp.
12. Wright, E.H.M., Adsorption of Methyl Laurate and Related Methyl Esters from Solution by Oxide Absorbents, *Trans. Faraday Soc. 61*:1764–1770 (1965).
13. Standard Test Method for Determination of the Coefficient of Friction of Lubricants Using the Four-Ball Wear Test Machine, *Annual Book of ASTM Standards 5*:164–167 (2001), D 5183-95.
14. Kingsbury, E.P., The Heat of Adsorption of a Boundary Lubricant, *ASLE Trans. 3*:30–33 (1960).
15. Frewing, J.J., The Heat of Adsorption of Long-Chain Compounds and Their Effect on Boundary Lubrication, *Proc. R. Soc. Lond. A 182*:270–285 (1944).
16. Sharma, J.P. R.C. Malhotra, and A. Cameron, Heat of Adsorption and Critical Temperature Studies of Boundary Lubricants on Steel Surfaces, *Wear 25*:281–297 (1973).
17. Cowley, C.W., C.J. Ultee, and C.W. West, Influence of Temperature on Boundary Lubrication, *ASLE Trans. 1*:281–286 (1958).
18. Huheey, J.E., E.A. Keiter, and R.L. Keiter, *Inorganic Chemistry,* Harper Collins College, New York, 1993.
19. Mori, S., and Y. Imaizumi, Adsorption of Model Compounds of Lubricant on Nascent Surfaces of Mild and Stainless Steels Under Dynamic Conditions, *Trib. Trans. 31*:449–453 (1988).
20. Miller, R., V.B. Fainerman, E.V. Aksenenko, V.V. Makievski, J. Kragel, L. Liggieri, F. Ravera, R. Wustneck, and G. Loglio, Surfactant Adsorption Kinetics and Exchange of Matter for Surfactant Molecules with Changing Orientation Within the Adsorption Layer, *Proceedings of the Symposium on Emulsions, Foams, and Thin Films* (University Park, PA, June 21–24, 1998), Marcel Dekker, New York, 2000, pp. 313–327.
21. Fukuzaki, S., H. Urano, and M. Hiramatsu, Study of the Conformation of Protein Adsorbed on Stainless Steel Surfaces, *J. Surface Finishing Jpn. 49*:1237–1238 (1998).

[Received December 10, 2004; accepted March 24, 2005]